New Journal of Physics
The open access journal at the forefront of physics

Deutsche Physikalische Gesellschaft DPG IOP Institute of Physics

OPEN ACCESS

The dynamics of macroparticles in a direct current glow discharge plasma under micro-gravity conditions

To cite this article: A P Nefedov *et al* 2003 *New J. Phys.* **5** 108

View the article online for updates and enhancements.

You may also like

- Analytical model of the breakdown mechanism in a two-phase mixture
Ye Qizheng, Li Jin and Xie Zhihui
- 2D axial-azimuthal particle-in-cell benchmark for low-temperature partially magnetized plasmas
T Charoy, J P Boeuf, A Bourdon et al.
- Kinetic theory of particle-in-cell simulation plasma and the ensemble averaging technique
Michaël Touati, Romain Codur, Frank Tsung et al.

This content was downloaded from IP address 194.95.157.36 on 27/01/2025 at 13:43

New Journal of Physics
An Institute of Physics and Deutsche Physikalische Gesellschaft Journal

The dynamics of macroparticles in a direct current glow discharge plasma under micro-gravity conditions

A P Nefedov[1], O S Vaulina[1], O F Petrov[1], V I Molotkov[1], V M Torchinskii[1], V E Fortov[1], A V Chernyshev[1], A M Lipaev[1], A I Ivanov[2], A Yu Kaleri[2], Yu P Semenov[2] and S V Zaletin[3]

[1] Institute of Thermal Physics of Extremal States, Russian Academy of Sciences, Moscow 127412, Russia
[2] Korolev Space Rocket 'Energiya' Corporation, Korolev, Moscow oblast 141070, Russia
[3] Gagarin Centre for Training Cosmonauts, Zvezdnyi gorodok, Moscow oblast 141160, Russia
E-mail: ofpetrov@ihed.ras.ru

New Journal of Physics **5** (2003) 108.1–108.11 (http://www.njp.org/)
Received 26 February 2003
Published 18 August 2003

Abstract. The dynamics of large-sized (70–180 μm) spherical bronze particles in a direct current glow discharge plasma was studied experimentally under microgravitation conditions. The temperatures, velocities, pair correlation functions and self-diffusion coefficients of macroparticles were measured at various discharge currents. The charges of dust particles (on the order of 10^6 e) corresponded to high surface potentials of about 30–40 V.

Contents

PII: S1367-2630(03)60150-3
© IOP Publishing Ltd and Deutsche Physikalische Gesellschaft

1. Introduction

A dust plasma is a partially ionized gas containing charged substance particles (dust) of micron dimensions. The size of dust particles allows them to be recorded on a videotape, which significantly simplifies the use of direct contactless methods for their diagnostics. A dust plasma is therefore a convenient experimental model for studying various transport phenomena in systems of interacting particles, such as charging and mass transfer, the formation of dust structures and complex oscillatory modes, etc [1]–[10]. In recent years, considerable attention has been given to experimental studies of dust plasmas under microgravitation conditions [6]–[10]. Such experiments allow a wide range of phenomena that cannot be observed in laboratories on the earth to be studied [6]–[8]: photoemission charging of aerosols in the upper layers of the atmosphere, ambipolar diffusion, the dynamics of large-size (larger than 100 μm) dust particles in a plasma, etc. Recent experiments performed by the Russian–German team on the International Space Station revealed the occurrence of several new phenomena in an RF discharge plasma, such as 'dust beats', the formation of plasma crystal with lattices of different types, opposite charging of macroparticles, etc. No analogues of such processes are observed under usual laboratory conditions [10].

In this work, we describe some of the earliest experiments on the dynamics of macroparticles under microgravitation conditions performed aboard the Mir space station during the 28th orbital expedition. The experiments were performed for large-size ($\sim$100 μm) bronze particles in a direct current glow (dc-) discharge plasma.

2. Experimental details

The experimental unit is schematically shown in figure 1. The main element of the working chamber was a gas discharge tube of radius $R_t = 1.6$ cm filled with neon (Ne) to a pressure of $P = 1$ Torr. The distance between a plane anode and a cathode was 28 cm. An insulated electrode was mounted at 4.5 cm from the anode. The electrode was made as two steel grids (wire 60 μm in diameter) with 150 μm $\times$ 150 μm meshes, and the distance between the grids was 1 cm. During experiments, the electrode was under a floating potential and prevented negatively charged macroparticles from escaping to the anode. Bronze spherical particles (particles 70–180 μm in diameter, mean radius $a = 62.5$ μm, density of the material $\rho = 8.2$ g cm^{-3}) were placed between the grid electrode and the cathode. The diagnostics of macroparticles was performed with the use of a plane laser beam ('laser knife' about 300 μm wide, wavelength 0.67 μm) and additional illumination of the dust cloud by an incandescent lamp. In the latter case, the number of detected particles was determined by the depth of field of the video system, which allowed us to keep track of particle positions for long enough to analyse their transport characteristics. The image was recorded on a video tape at a 50 s^{-1} frame frequency. The video data were processed using a special program for identifying the displacements of separate particles in the visual field of video recording.

Experiments were performed at discharge currents ($I = 0.1$–0.8 mA) varied by the current source. Bronze particles were initially situated on the tube walls. For this reason, the system was subjected to a dynamic action (pushed) after switching on a discharge to shake off particles from the tube walls. After the dynamic action, bronze particles moved toward the insulated grid electrodes, in the vicinity of which ordered structures were formed (figures 2(a), (b)). The discharge was then 'quenched', the particles relaxed to the initial state (returned to the tube walls),

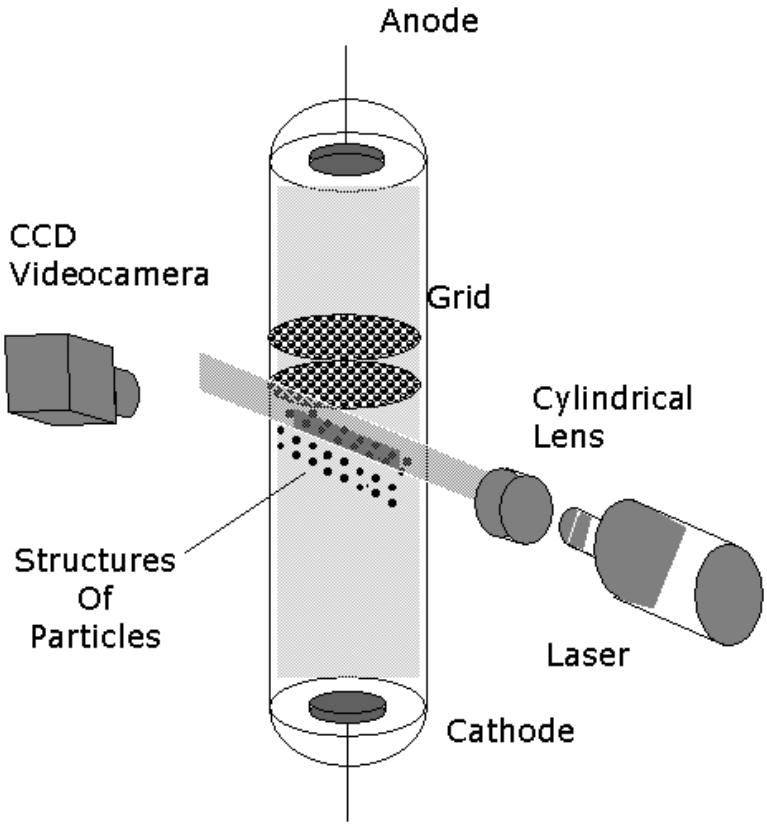

Figure 1. Schematic drawing of the experimental unit.

and the experiment was repeated at a new gas discharge current value. Plasma concentration $n_0 \approx n_e^0 \approx n_i^0$ (here $n_{e(i)}^0$ is the concentration of electrons (ions) in the absence of dust particles) in the region of the positive discharge column can be estimated from discharge current density measurements, $j = I/\pi R_t^2 \approx 12$–$96\ \mu\text{A cm}^{-2}$; this value should remain constant over the whole tube length:

$$j = e\mu_e E n_e^0, \tag{1}$$

where μ_e is the mobility of electrons (for neon, $\mu_e P \approx 1.5 \times 10^6$ Torr cm^2 V^{-1} s^{-1}). In tubes with radii of 1–2 cm and $P = 1$ Torr, field E of the positive column in a normal glow discharge in neon is $E \sim 1$ V cm^{-1}, the normal current density is $j_n = 5$–$6\ \mu\text{A cm}^{-2}$, and the mean electron energy characterizing electron temperature T_e is about 3–5 eV [11]. Under our experimental conditions, discharges occurred in an anomalous mode (which followed from both the recorded current densities and current–voltage characteristics), and the electric field strength obeyed the equation $E \propto j^{1/2}$ [11]. At $E = 1.5$ V cm^{-1} and $j = 12\ \mu\text{A cm}^{-2}$, the mean plasma concentration calculated by (1) was $n_0 = (5$–$14) \times 10^7$ cm^{-3} ($j = 12$–$96\ \mu\text{A cm}^{-2}$). Taking into account the Bessel radial profile, the plasma density along the tube axis, where the parameters of dust particles were measured, reached values on the order of $2.4n_0$ [11]. The further estimates will therefore be based on the assumption that, in the absence of particles, the concentration of electrons (ions) varied in the range 10^8 cm^{-3} under current density variations from 12 to 96 μA cm^{-2}.

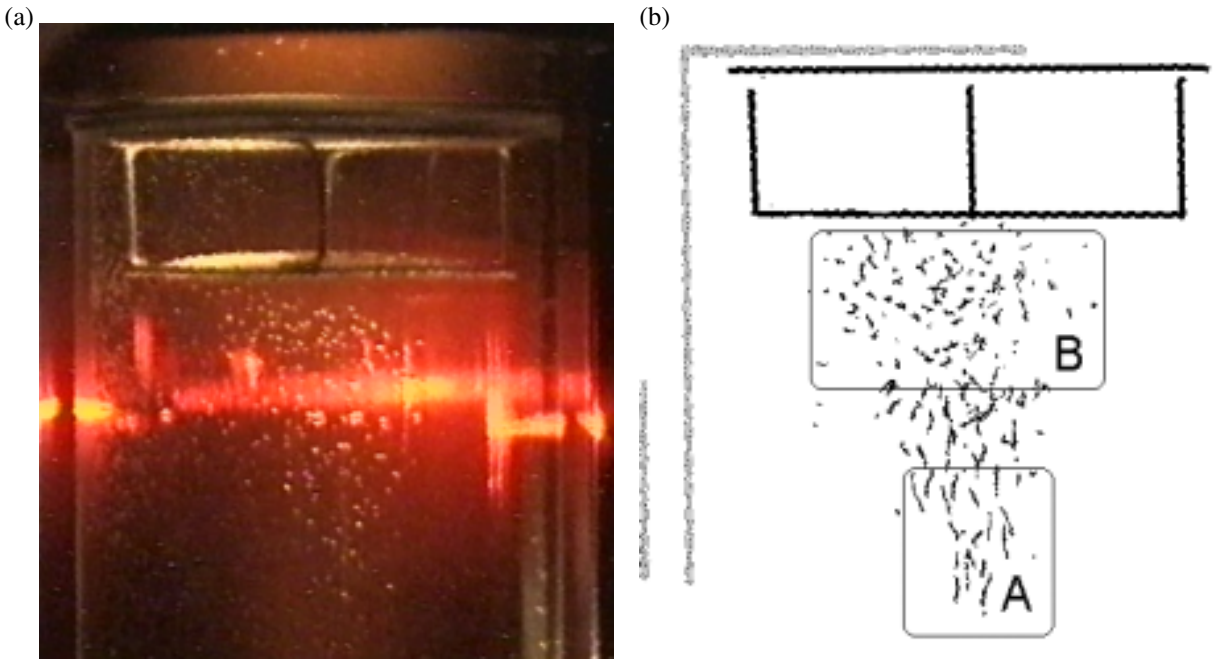

Figure 2. Video images of (a) gas-discharge tube and (b) particle trajectories from the discharge positive column toward the insulated grid electrodes.

3. Measurement results and their analysis

The determination of dust charges from the drift velocity of macroparticles

The mean drift velocity V_p of particles from the positive column (figure 2(b), field A) to the grid electrode is shown in figure 3 as a function of discharge current I. As the velocity of particle motions in the measurement volume remained virtually constant, their charges eZ_p could be found from the equation of motion [8]

$$m_p \, dV_p/dt = -\nu_{fr} m_p V_p + EeZ_p \equiv 0, \tag{2}$$

where m_p is the mass of the particle and ν_{fr} is the friction coefficient of dust particles, which determines the frequency of their collisions with surrounding gas neutrals [12, 13],

$$m_p \nu_{fr} = 6\pi a \eta (1 - l_g(1 - \exp(-2a/l_g))/2a). \tag{3}$$

Here, $l_g(\mu\text{m/Torr}) \approx 125/P$ is the free path of neon neutrals and $\eta \approx 3.17 \times 10^{-4}$ g cm^{-1} s^{-1} is the viscosity of neon at $l_g \ll a$. Setting E (V cm^{-1}) $= 1.5(j$ (μA cm^{-2})$/12)^{1/2}$ and $a = 62.5$ μm in (2) and (3), we find that particle charge $Z_p \approx 10^6$ is virtually independent of discharge current (figure 4, curve 1) and corresponds to fairly high surface potentials $\varphi_s = eZ_p/a_p \approx 35$–$37$ V. The errors in the φ_s values obtained by this method are determined by the availability of *a priori* information on the field and friction coefficient values in (2).

The formation of liquid dust structures

The characteristic dimensions of dust clouds formed in the vicinity of the grid electrode (figure 2(b), field B) were about 2 cm in the radial direction and 0.7–1.3 cm from the grid edge

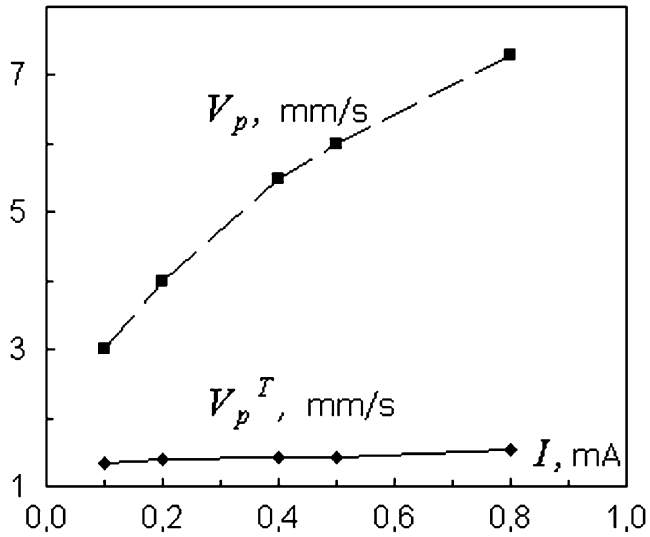

Figure 3. Mean thermal and drift V_p velocities of particles from the positive column region (figure 2(b), field A) to grid electrodes at various discharge currents I.

along the tube axis. Pair correlation functions $g(l)$ for various discharge currents I are shown in figure 5. At low I values, the degree of ordering of particles in the dust cloud increases as their concentration n_p grows. An increase in n_p is accompanied by a decrease in $l_\mathrm{max} \approx l_\mathrm{p} = n_\mathrm{p}^{-1/3}$, where l_max is the position of the main $g(l)$ maximum and l_p is the mean interparticle distance. The mean interparticle distance l_p was changed from ~750 to ~1000 μm. Because of a fairly small number of particles in the laser knife plane, a quantitative analysis of the experimental $g(l)$ functions is virtually impossible. Nevertheless, the presence of fairly well-defined secondary $g(l)$ maxima is evidence of strong interparticle interactions and weak screening of particles (screening parameter $\kappa = l_\mathrm{p}/\lambda < 1$, where λ is the screening length).

According to the Lindemann criterion, a solid phase melts if the ratio between the root of the mean-square displacement Δ_0 of particles from their equilibrium positions and the mean interparticle distance l_p reaches about 0.15 [14]. In experiments, particle displacements are usually measured from the centre of mass of the system, that is $\Delta = \sqrt{2}\Delta_0$, and the Lindemann parameter at the melting curve is therefore $\delta_\mathrm{c} = \Delta/l_\mathrm{p} \approx 0.21$. The $\delta_\mathrm{c}(t) = \Delta_N(t)/l_\mathrm{p}$ time dependence (here, $\Delta_N(t) = \sqrt{\langle(\boldsymbol{l}(t) - \boldsymbol{l}(0))^2\rangle_N}$: $\boldsymbol{l}(t)$ is the displacement of a separate particle and $\langle\ \rangle_N$ denotes averaging over the ensemble of N particles) for 16 particles ($N_\mathrm{p} = 16$), which remain in the visual field of the video system for about 4.5 s, is shown in figure 6(a). Note that, during some time intervals, the $\Delta_N(t)/l_\mathrm{p}$ ratio remains constant and corresponds to the Lindemann criterion. When the observation time was decreased to about 1 s, the number of identified trajectories increased to $N_\mathrm{p} = 70$–120 at the expense of particles that experienced transitions between 'settled' states from one cloud region to another. Averaging of particle displacements $\Delta_N(t)$ over the ensemble was then close to time averaging, $\Delta_N^t = \sqrt{\langle\langle(\boldsymbol{l}(t) - \boldsymbol{l}(0))^2\rangle_N\rangle_t}$ (figure 6(a)). Here, $\langle\ \rangle_{N,t}$ denotes averaging over the ensemble and time, respectively. A similar picture was observed in numerical simulations of the dynamics of macroparticles with the Yukawa interaction potential $\varphi = eZ_\mathrm{p}\exp(-l/\lambda)/l$ in a strongly nonideal dust liquid [15]. 'Jumps' observed in simulated systems are illustrated by figure 6(b),

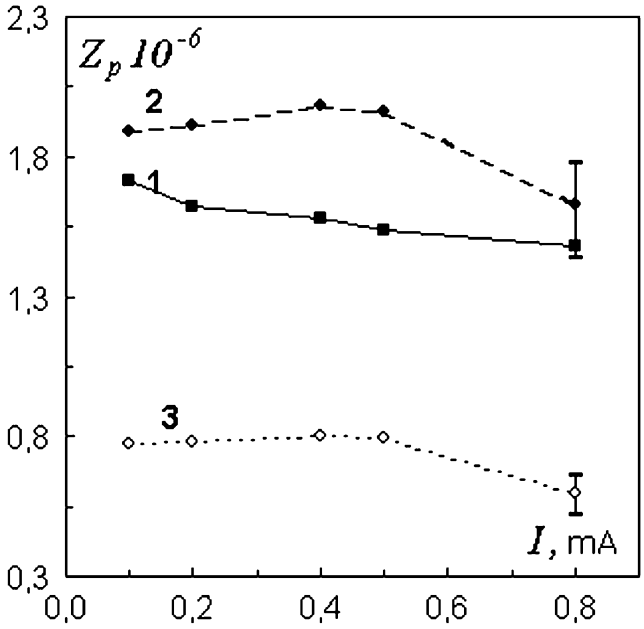

Figure 4. Particle charge Z_p as a function of discharge current I (1) obtained from equation of motion equation (2) for $a = 62.5\ \mu$m, (2) diffusion measurements by equations (5) and (6) for $a = 62.5\ \mu$m, and (3) diffusion measurements for $a = 35\ \mu$m.

where the difference between the ensemble Δ_N/l_p and time Δ_N^t/l_p averages close to the crystallization curve of the system, where the Γ^* normalized nonideality parameter tends to 102, is shown. This difference vanishes as Γ^* decreases, and the system under study becomes ergodic.

The Γ^* normalized parameter value determines the degree of ordering and the dynamics of particles in nonideal Yukawa systems [15, 16],

$$\Gamma^* = (1 + \kappa + \kappa^2/2)\exp(-\kappa)\Gamma, \tag{4}$$

where $\kappa = l_p/\lambda$, $\Gamma = (eZ_p)^2 n_p^{1/3}/T_p$. Here, T_p is the temperature of macroparticles in energy units.

Diffusion of macroparticles

The self-diffusion coefficient of macroparticles D_p can be found from measured mean-square displacements from

$$D(t) = \langle\langle(\boldsymbol{l}(t) - \boldsymbol{l}(0))^2\rangle_N\rangle_t/6t. \tag{5}$$

The relation between the D_p self-diffusion coefficient given by $D_p = \lim_{t\to\infty} D(t)$ and the Γ^* value (4) in strongly correlated ($\Gamma^* > 30$) Yukawa systems can be written as [16]

$$D_p \cong \frac{T_p\Gamma^*}{12\pi(\omega_l + \nu_{fr})m_p}\exp\left(-3\frac{\Gamma^*}{\Gamma_c}\right), \tag{6}$$

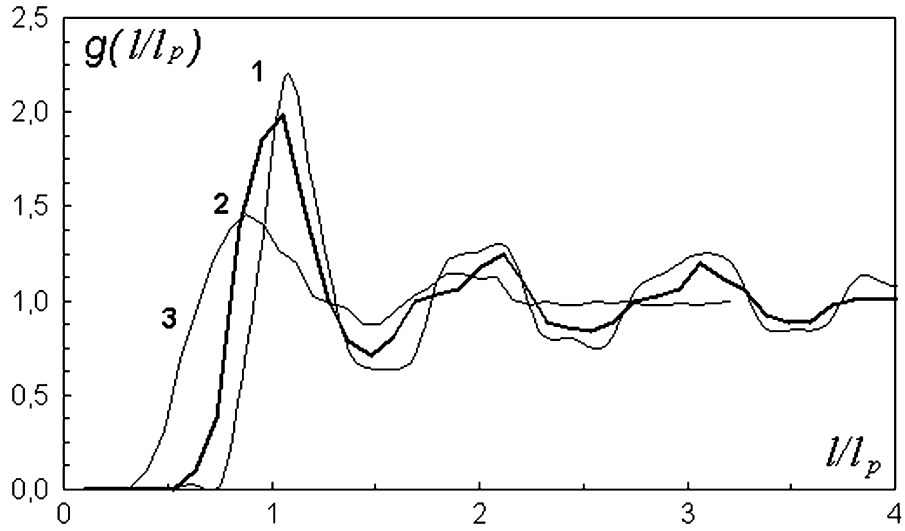

Figure 5. Pair correlation functions $g(l/l_p)$ versus l/l_p for dust structures formed close to grid electrodes (figure 2(b), field B) at discharge currents I of (1) 0.1 mA, (2) 0.4 mA, and (3) 0.8 mA.

where $\Gamma_c \approx 102$ is the Γ^* parameter value at the crystallization point and $\omega_l = eZ_p(n_p/\pi m_p)^{1/2}(1+\kappa+\kappa^2/2)^{1/2}\exp(-\kappa/2) \equiv (\Gamma^* T_p/\pi l_p^2 m_p)^{1/2}$ is the normalized dust frequency. The error involved in approximation (6) sharply decreases as Γ^* increases; it amounts to about 30% for $\Gamma^* \approx 30$ and less than 3% at $\Gamma^* > 50$ [15]. Equation (6) allows Γ^* to be determined fairly easily from the results obtained in measurements of the mean interparticle distance l_p, temperature T_p, and the D_p diffusion coefficient of macroparticles. In our experiments the $l_p \approx 700$–1000 μm, and $D_p \approx 0.1$–1.1 mm^2 s^{-1} values were increased by the discharge current I. The value of diffusion coefficient for noninteracting particles ($D_0 = T_p/m_p\nu_{fr}$) was found to be more than an order of magnitude larger than the D_p value calculated by (5). The dust temperature T_p was about 10^5 eV. The temperature of macroparticles was established by finding the Maxwell distribution that best described the recorded spectrum of instantaneous velocities of particles obtained by analysing video records. A similar procedure for determining temperature was described in [2, 7]. The mean velocities of chaotic movement of particles were about 1 mm s^{-1} (see figure 3). Note that this procedure could underestimate the mean chaotic energy of particles (kinetic temperature) if the frame frequency w (50 s^{-1} in our experiments) did not satisfy the condition $w \gg \nu_{fr}$ [2].

The nonideality parameter and macroparticle charges

The Γ^* normalized parameter values reproduced by (6) from diffusion coefficient measurements are shown in figure 7 for the mean ($a = 62.5$ μm) and minimal ($a_{min} = 35$ μm) particle sizes. Note that Γ^* determinations are only based on measurement results. The ν_{fr} friction coefficient value depends on the radius of particles, but it does not significantly influence the Γ^* value because $\nu_{fr} < \omega_l$ under the experimental conditions. If the effects of screening macroparticles in a plasma–dust system are significant, an analysis of diffusion of macroparticles on the assumption of negligibly weak screening ($\Gamma^* = \Gamma, \kappa < 1$) gives a minimal estimate of the charge Z_p of

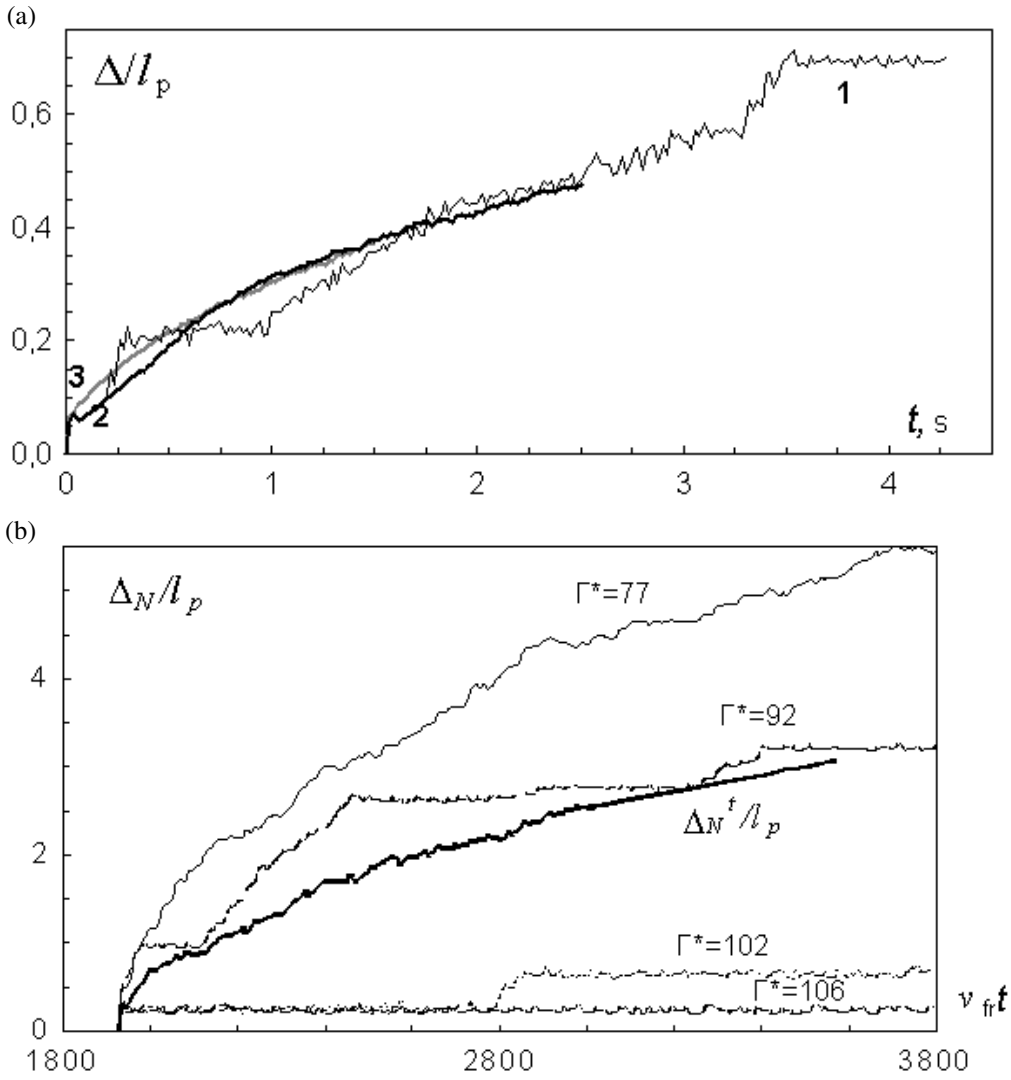

Figure 6. (a) Measurement time dependences of Lindemann parameter $\delta_c = \Delta(t)/l_p$ ($I = 0.4$ mA) obtained using various averaging techniques: (1) $\Delta(t) \equiv \Delta_N(t)$, $N_p = 16$; (2) $\Delta(t) \equiv \Delta_N^t(t)$, $N_p = 16$; (3) $\Delta(t) \equiv \Delta_N^t(t)$, $N_p = 96$. (b) 'Jumps' in simulated Yukawa systems (thick line corresponds to $\Gamma^* = 92$).

dust macroparticles irrespective of the form of the interparticle interaction potential. Parameter $\Gamma^* \approx \Gamma$ measurements for $\kappa = 0$ allow surface potentials at $I \leq 0.5$ mA to be determined. This gives $\varphi_s \approx 42$ V for medium-sized particles $a = 62.5$ μm and $\varphi_s \approx 30$ V for particles of radius $a_{min} = 35$ μm (see figure 4). For $I = 0.8$ mA, the recorded surface potential value is lower by approximately 30%. The error in determining the charge of macroparticles is then substantially larger, because at low $\Gamma^* < 35$ values, (6) is fairly inaccurate (see figure 7). The obtained macroparticle charge estimates are in agreement with the results of determining Z_p from the equation of motion (2). We can therefore hope that the surface potentials $\varphi_s \approx 30$–42 V ($I \leq 0.5$ mA) and $\varphi_s \approx 22$–30 V ($I = 0.8$ mA) correctly reproduce the real Z_p charge values, and, accordingly, the assumption of weak screening ($\kappa < 1$) of macroparticles corresponds well with the conditions existing in the dust system under study.

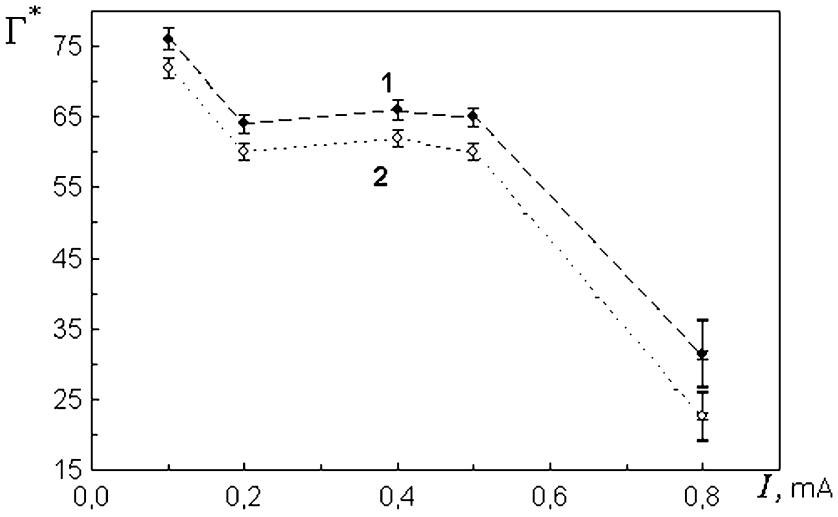

Figure 7. Normalized nonideality parameters Γ^* reproduced from diffusion coefficient measurements for particles of different sizes: (1) $a = 62.5\ \mu$m and (2) $a_{\min} = 35\ \mu$m; error intervals for reproducing Γ^* by (4) are shown.

According to the orbit motion limited (OML) theory, the particle charge $Z_p = zaT_e/e^2$, where $z \approx 2$–4 for most of the experimental conditions in a direct current glow discharge [17, 18]. Note that, in the presence of large-size particles with $a > 10$–$20\ \mu$m, the mean free path l_i of ions (Ar, Ne) at room temperature becomes comparable with or smaller than a [11] and typical buffer gas pressures $P \approx 1$ Torr. This decreases flow of ions onto the surface of a dust particle and, therefore, increases φ_s and z. A similar effect was observed experimentally. For instance, it was shown in [8] that the surface potential of a particle grew approximately from 9 to 30 V as the particle radius increased from 2 to 7 μm in neon at $P \approx 0.5$–1.5 Torr. This corresponded to changes in z approximately from 3 to 10 at $T_e = 3$ eV. Thus we can assume that the dust surface potentials $\varphi_s = zT_e/e$ can attain ~30–50 V under the conditions of our experiments ($a \sim 30$–$90\ \mu\text{m} > l_i \sim 10$–$20\ \mu$m) because the electron temperature is $T_e \sim 3$–5 eV for direct current glow discharges in neon [11].

Note also that high macroparticle charges $Z_p \approx 10^6$ at their concentrations $n_p \approx 10^3$ cm^{-3} do not correspond with the suggestion of the electroneutrality of the system, $Z_p n_p + n_e = n_i$, if we assume that the presence of dust particles have no significant influence on discharge conditions and the concentration of ions in the dust cloud is comparable with their concentration in the absence of macroparticles, $n_i^0 \approx 10^8$ cm^{-3}. Such a discrepancy has already been observed in laboratory conditions on the earth. For instance, heavy glass particles hovered in weak fields (about 1–12 V cm^{-1}) of glow discharge strata and positive columns in neon [19], which led the authors of [19] to suggest either the existence of higher charges Z_p or a sharp increase in electric field E caused by a change in the discharge conditions in the dust cloud.

The influence of macroparticles on equilibrium ionization

The influence of macroparticles on kinetic processes in a glow discharge can be substantial, because a considerable decrease in the concentration n_e of electrons as a consequence of their effective loss on dust cloud particles results in an increase in electric field strength

(j = constant $\rightarrow$ En_e = constant). The mean electron energy then increases, which causes an increase in ionization frequency ν_i, which in turn increases the concentration of electrons to its equilibrium value.

As glow discharges in rare gases are usually controlled by ambipolar diffusion (plasma recombination on gas-discharge tube walls), this sequence is only observed if the electron loss frequency ν_{ep} on dust cloud particles is comparable with or much larger than the ν_{ab} frequency of diffusion electron loss [11],

$$\nu_{ab} \cong (2.4)^2 D_a / R_{tr}^2, \tag{7}$$

where $D_a \cong \mu_i T_e / e$ is the ambipolar diffusion coefficient at $T_e \gg T_i$, and $\mu_i \approx 3200\,\mathrm{cm^2\ V^{-1}\ s^{-1}}$ is the mobility of singly charged ions in neon at $P = 1$ Torr.

The ν_{ep} electron loss frequency on dust cloud particles can be estimated as

$$\nu_{ep} \cong (8\pi T_e / m_e)^{1/2} n_p a_p^2 \exp(-z). \tag{8}$$

Substituting the conditions of our experiments ($a = 62.5$ μm and $n_p = (1\text{–}3) \times 10^3$ cm^{-3}) into (8), we find that, at $z = 3$–4, the ν_{ep} electron loss frequency on dust cloud particles far exceeds the ν_{ab} diffusion loss frequency ($\nu_{ep}/\nu_{ab} > 10$ at $T_e < 15$ eV). We can therefore assume that discharge conditions in our experiments are determined by plasma recombination on the surface of particles.

Under steady state conditions, the rate of electron loss should be compensated by the rate of particle creation, and, accordingly, the ionization frequency ν_i should coincide with the electron loss frequency. Note that, in a positive column free of particles, ionization equilibrium is attained by equalizing the rates of plasma ionization ($n_e^0 \nu_i$) and recombination on tube walls ($\beta_{ab} n_e^0 n_i^0$):$n_e^0 \nu_i \equiv n_e^0 \nu_{ab} = \beta_{ab} n_e^0 n_i^0$, and the condition of ionization equilibrium in a dust cloud is $n_e \nu_i \equiv n_e \nu_{ep} = \beta_{ep} n_e n_i$, where β_{ab} and β_{ep} are the corresponding recombination coefficients. Suppose that the plasma recombination coefficients on tube walls and on the surface of dust particles are approximately equal, $\beta_{ab} \approx \beta_{ep}$. The ratio between the n_i concentration of ions in a dust cloud and the n_i^0 concentration of ions in a plasma without macroparticles is then given by

$$n_i / n_i^0 \equiv \nu_{ep} / \nu_{ab}, \tag{9}$$

where the $n_i^0 \approx (1\text{–}3) \times 10^8$ cm^{-3} value corresponds to the experimental current density. Using (9) and taking into account (7) and (8), we find that $n_i \approx (5\text{–}7.5) \times 10^9$ cm^{-3} at various discharge currents already at $z = 4$. At $z = 3$, n_i is approximately three times smaller. The condition $Z_p n_p < n_i$ necessary for the confinement of negatively charged particles is therefore quite attainable in the plasma–dust system under consideration. Note once more in conclusion that plasma parameter estimates considered in this section are used to analyse a qualitative picture of the influence of particles on ionization processes under the conditions of a dense dust cloud.

4. Conclusion

This work describes the results of experimental studies of the dynamics of bronze macroparticles in a dc-discharge plasma under microgravitation conditions. The temperatures, concentrations, pair correlation functions, self-diffusion coefficients, and charges of macroparticles were measured in various discharge currents. An analysis of the measurement results showed that the observed structures of macroparticles corresponded to a strongly nonideal dust liquid

($\Gamma^* \sim 60$–75), and their dynamics was in close agreement with the results of simulating Yukawa systems characterized by weak screening ($\kappa < 1$).

Experimental estimates of macroparticle charges corresponded to surface potentials of the order of 30–40 V, which far exceeded values predicted by the OML theory. This discrepancy could be related to both a decrease in the effective flow of ions onto particles whose radii were larger than the free path of ions and an increase in the temperature of electrons in the dust cloud because of an influence of macroparticles on equilibrium ionization in dc-discharge.

Note once more in conclusion that experiments on studying interaction potentials and charging processes for large-size 100 μm particles in a dust plasma cannot be performed under earth gravitation conditions.

Acknowledgments

The authors are deeply indebted to astronauts S V Avdeev, Yu M Baturin, T A Musabaev and G I Padalka for much work done to prepare the 'Plazmennyi Kristall-2' cosmic experiment aboard the 'Mir' orbital station. This work was financially supported by the Russian Foundation for Basic Research (project no 01-02-16658) and INTAS (project no 2001-0391).

References

[1] Thomas H *et al* 1994 *Phys. Rev. Lett.* **73** 652
[2] Melzer A, Homann A and Piel A 1996 *Phys. Lett.* A **53** 2757
[3] Zhakhovsky V V *et al* 1997 *Pis. Zh. Eksp. Teor. Fiz.* **66** 392 (Engl. transl. 1997 *JETP Lett.* **66** 419)
[4] Nunomura S, Misawa T, Ohno N and Takamura S 1999 *Phys. Rev. Lett.* **83** 1970
[5] Vaulina O *et al* 1999 *Phys. Rev.* E **60** 5959
[6] Fortov V E *et al* 1998 *Zh. Eksp. Teor. Fiz.* **114** 2004 (Engl. transl. 1998 *JETP* **87** 1087)
[7] Vaulina O S *et al* 2001 *Zh. Eksp. Teor. Fiz.* **119** 1129 (Engl. transl. 2001 *JETP* **92** 979)
[8] Fortov V E *et al* 2001 *Phys. Rev. Lett.* **87** 205002
[9] Morfill G *et al* 1999 *Phys. Rev. Lett.* **83** 1598
[10] Stuffler T *et al* 2001 *Proc. 52nd Int. Astronautical Congr. (Toulouse, France 2001)* IAF-01-J.6.02
[11] Raizer Yu P 1987 *Gas Discharge Physics* (Moscow: Nauka)
[12] Lifschitz E M and Pitaevskii L P 1981 Physical kinetics *Course of Theoretical Physics* vol 10, ed L D Landau and E M Lifschitz (Oxford: Pergamon)
[13] Fuchs N A 1964 *The Mechanics of Aerosols* (New York: Dover)
[14] Lindemann F A 1910 *Z. Phys.* **11** 609
[15] Vaulina O S and Vladimirov S V 2002 *Plasma Phys.* **9** 835
[16] Vaulina O S and Khrapak S A 2001 *Zh. Eksp. Teor. Fiz.* **119** 264 (Engl. transl. 2001 *JETP* **92** 228)
[17] Vaulina O S, Khrapak S A, Samarian A A and Petrov O F 2000 *Phys. Scr.* **84** 292
[18] Goree J 1994 *Plasma Sources Sci. Technol.* **3** 400
[19] Lipaev A M *et al* 1997 *Zh. Eksp. Teor. Fiz.* **112** 2030 (Engl. transl. 1997 *JETP* **85** 1110)